
PARTITIONING ISRAELI MUNICIPALITIES INTO POLITICALLY HOMOGENEOUS CANTONS: A CONSTRAINED SPATIAL CLUSTERING APPROACH

A PREPRINT

Adir Elmakais
Department of Computer Science
Bar-Ilan University
Ramat Gan, Israel
adir.elmakais@live.biu.ac.il

Oren Glickman
Department of Computer Science
Bar-Ilan University
Ramat Gan, Israel
oren.glickman@biu.ac.il

March 2026

ABSTRACT

Israeli society has experienced significant political polarization in recent years, reflected in five Knesset elections held within a four-year period (2019–2022). Public discourse increasingly references hypothetical divisions of the country into politically homogeneous "cantons." This paper develops a data-driven algorithmic approach to explore such divisions using publicly available municipality-level election results and geographic boundary data from the Israel Central Bureau of Statistics.

We partition 229 Israeli municipalities into geographically contiguous cantons that maximize internal political similarity. Our methodology employs four clustering algorithms—Simulated Annealing, Agglomerative Clustering with contiguity constraints, Louvain Community Detection, and K-Means (baseline)—evaluated across four feature representations (BlocShares, RawParty, PCA, NMF), three distance metrics (Euclidean, Cosine, Jensen-Shannon), and six values of K (3–20), yielding 264 experimental configurations.

Key results show that BlocShares with Euclidean distance and Agglomerative clustering produces the highest clustering quality (silhouette score 0.905), while NMF with Louvain community detection achieves the best balance between political homogeneity, silhouette quality (0.121), and interpretable canton assignments. Temporal stability analysis across all five elections reveals that deterministic algorithms produce near-perfectly stable partitions (ARI up to 1.0), while Israel’s political geography remains structurally consistent despite electoral volatility. The resulting $K=5$ partition identifies five politically coherent regions—a center-leaning metropolitan core, a right-wing southern arc, a right-leaning northern mixed region, and two Arab-majority cantons—closely reflecting known political-demographic divisions. An interactive web application accompanies this work.

Keywords spatial clustering · political geography · electoral analysis · Israel · constrained partitioning · community detection

1 Introduction

1.1 Motivation

Over the past four years, Israel held five Knesset elections (April 2019, September 2019, March 2020, March 2021, and November 2022), an unprecedented frequency that reflects deep political divisions across multiple dimensions: secular versus religious, left versus right on the ideological spectrum, Arab versus Jewish communal politics, and attitudes toward judicial reform and governance. Throughout this period, public and media discourse repeatedly invoked the notion of dividing Israel into separate “cantons” along political lines—contrasting, for example, Tel Aviv’s liberal-

secular majority with Jerusalem’s religious-conservative population, or the Arab-majority towns of northern Israel with predominantly Jewish communities elsewhere.

While such discourse is largely rhetorical, it raises a compelling computational question: if Israel were to be divided into politically coherent regions based purely on voting patterns, what form would those regions take, and how stable would they be across election cycles? This paper applies data-driven computational methods to answer this question rigorously.

1.2 Research Objectives

This work has three primary objectives:

1. **Partition 229 Israeli municipalities into K geographically contiguous cantons** that maximize internal political homogeneity, using municipality-level election results from five Knesset elections.
2. **Systematically compare clustering approaches** across multiple feature representations, distance metrics, algorithms, and values of K , evaluating trade-offs between political homogeneity, population balance, and geographic compactness.
3. **Analyze the temporal stability** of canton boundaries across election cycles to determine whether Israel’s political geography is structurally persistent or volatile.

1.3 Contributions

This paper makes the following contributions:

- A novel application of constrained spatial clustering to Israeli political geography, combining graph-based contiguity constraints with political feature-space optimization.
- A comprehensive experimental framework evaluating 264 configurations across four representations, three distance metrics, four algorithms, and six values of K .
- Temporal stability analysis across five elections using Adjusted Rand Index (ARI) and Normalized Mutual Information (NMI).
- Qualitative case studies validating that algorithmic cantons align with known political-demographic divisions.
- An interactive web application for exploring canton partitions, experiment results, and stability analysis.¹
- An open-source, modular Python codebase enabling reproducible analysis and extension.²

1.4 Paper Outline

Section 2 reviews related work. Section 3 formally defines the constrained canton partitioning problem. Section 4 describes the data sources and processing pipeline. Section 5 presents the methodology. Section 6 reports experimental results. Section 7 analyzes temporal stability. Section 8 presents qualitative case studies. Section 9 discusses limitations and future work, Section 10 addresses ethical considerations, and Section 11 concludes.

2 Related Work

2.1 Electoral Redistricting and Gerrymandering

The problem of dividing a territory into politically meaningful regions has deep connections to electoral redistricting research. In democratic systems with district-based representation, electoral boundaries must be periodically redrawn to reflect population changes, and the drawing process can be manipulated to favor particular parties—a practice known as gerrymandering [Stephanopoulos and McGhee, 2015].

Brieden et al. [2017] proposed a constrained clustering approach to electoral redistricting based on generalized Voronoi diagrams and linear programming. Their method partitions geographic units into districts with hard population balance constraints while minimizing intra-district political heterogeneity.

¹<https://israel-cantons-project-5j7kgq8acxrbiflraqnhgb.streamlit.app/>

²<https://github.com/adirelm/israel-cantons-project>

Our work differs from classical redistricting in important ways: (1) we aim to *maximize* political homogeneity within cantons, whereas fair redistricting often seeks competitive or balanced districts; (2) we operate at the municipality level rather than individual census blocks; and (3) our work is purely descriptive and exploratory rather than prescriptive. However, the shared technical challenges—ensuring geographic contiguity, handling population constraints, and operating on spatial graphs—make redistricting research directly relevant.

Recent computational approaches to fair redistricting include Markov Chain Monte Carlo methods that sample from the space of valid partitions to detect gerrymandering outliers [DeFord et al., 2021], and graph-based metrics for measuring district compactness [Duchin and Tenner, 2018].

2.2 Spatial and Constrained Clustering

Standard clustering algorithms—K-Means, hierarchical agglomerative methods, spectral clustering—operate in feature space without regard to geographic structure [Hastie et al., 2009]. When geographic contiguity is required (as in regionalization), these methods must be extended with spatial constraints.

Spatially-constrained agglomerative clustering is a natural approach: starting with each spatial unit as its own cluster, iteratively merge adjacent clusters that are most similar in feature space [Murtagh and Legendre, 2014]. Spectral clustering leverages the graph Laplacian to embed graph nodes into a low-dimensional space before applying K-Means [von Luxburg, 2007].

Community detection algorithms from network science, particularly the Louvain method [Blondel et al., 2008], offer an alternative by maximizing modularity [Newman and Girvan, 2004]. Metaheuristic approaches such as Simulated Annealing can optimize arbitrary multi-objective cost functions over the partition space while maintaining contiguity through constrained neighborhood operations [Kirkpatrick et al., 1983].

2.3 Political Geography of Israel

Israel’s political landscape is characterized by several cross-cutting cleavages [Diskin and Diskin, 2005]: the left-right ideological spectrum, the secular-religious divide, the Arab-Jewish divide, and strong spatial autocorrelation—nearby municipalities tend to vote similarly due to shared demographics and social networks [Arian and Shamir, 2008, Shamir and Arian, 1999, Anselin, 1995]. This geographic structure makes Israel a suitable testbed for constrained spatial clustering.

2.4 Dimensionality Reduction for Voting Data

Municipality-level election data can be represented as high-dimensional vectors of party vote shares. Dimensionality reduction techniques compress these vectors while preserving key political structure: PCA finds orthogonal axes of maximum variance [Jolliffe, 2002], NMF decomposes vote shares into additive, interpretable “political archetypes” [Lee and Seung, 1999], and manual bloc aggregation groups parties into predefined political blocs, producing a low-dimensional but domain-informed representation.

2.5 Research Gap

Prior work on constrained spatial clustering has focused primarily on fair electoral redistricting—producing *competitive* districts with balanced partisan composition [Stephanopoulos and McGhee, 2015, Brieden et al., 2017, DeFord et al., 2021]. In contrast, our work seeks to maximize political *homogeneity* within regions. While regionalization methods such as SKATER [Assunção et al., 2006] and MAX-P-REGIONS [Duque et al., 2012] address spatially constrained partitioning, they have not been applied to Israeli political geography, nor evaluated across a systematic grid of feature representations, distance metrics, and algorithms. Existing studies of Israeli political geography [Arian and Shamir, 2008, Shamir and Arian, 1999] are primarily qualitative. This work bridges these gaps by combining constrained spatial clustering with a comprehensive experimental comparison tailored to the Israeli political context.

3 Problem Definition

3.1 Formal Statement

Let $V = \{v_1, \dots, v_n\}$ be a set of n municipalities, each characterized by a political feature vector $f_i \in \mathbb{R}^d$ derived from election results. Let $G = (V, E)$ be a geographic contiguity graph where edge (v_i, v_j) exists if municipalities i and j share a geographic boundary. Let w_i denote the voter population of municipality i .

The Canton Partitioning Problem: Given V , G , feature vectors $\{f_i\}$, voter weights $\{w_i\}$, and a target number of cantons K , find a partition $\mathcal{C} = \{C_1, \dots, C_K\}$ of V that:

1. **Maximizes political homogeneity:** Minimizes within-canton political variance.
2. **Ensures geographic contiguity:** Each canton C_k induces a connected subgraph of G .
3. **Balances population:** Minimizes disparity in total voter population across cantons.

This is a variant of the regionalization problem [Assunção et al., 2006, Duque et al., 2012].

3.2 Multi-Objective Formulation

These objectives may conflict. We adopt a weighted multi-objective approach:

$$\text{Cost}(\mathcal{C}) = \alpha \cdot \text{Homogeneity}(\mathcal{C}) + \beta \cdot \text{Balance}(\mathcal{C}) + \gamma \cdot \text{Compactness}(\mathcal{C}) \quad (1)$$

where α, β, γ are tunable weights. The three components are defined as:

- $\text{Homogeneity}(\mathcal{C}) = \sum_{k=1}^K \frac{|C_k|}{n} \cdot \overline{\text{Var}}(\mathbf{f}_i : i \in C_k)$, the population-weighted average of within-canton feature variance across dimensions.
- $\text{Balance}(\mathcal{C}) = \sigma(\mathbf{w})/\mu(\mathbf{w})$, the coefficient of variation of canton voter populations $\mathbf{w} = (w_1, \dots, w_K)$.
- $\text{Compactness}(\mathcal{C}) = |\{(u, v) \in E : C(u) \neq C(v)\}|/|E_{\text{assigned}}|$, the fraction of graph edges crossing canton boundaries (cut ratio), where E_{assigned} is the set of edges whose both endpoints have been assigned to a canton.

In our implementation, we use $\alpha = 0.4$, $\beta = 0.4$, $\gamma = 0.2$, reflecting equal priority for homogeneity and population balance with compactness as a secondary regularizer. Feature vectors are standardized (zero-mean, unit-variance) before cost computation.

3.3 Contiguity Constraint

The contiguity constraint requires that each canton C_k forms a connected subgraph of G . This is enforced structurally in agglomerative methods (only adjacent clusters merge) and algorithmically in SA (moves are rejected if they break contiguity).

4 Data Sources

4.1 Election Data

We use municipality-level election results from five consecutive Knesset elections, obtained from the Israel Central Bureau of Statistics (CBS) [Israel Central Bureau of Statistics, 2023a]. Table 1 summarizes the data scope.

Table 1: Municipality-level election data across five Knesset elections (all cover 229 municipalities).

Election	Knesset	Date	Eligible	Actual	Turnout
1	21	Apr. 2019	6,014,124	3,873,326	64.4%
2	22	Sep. 2019	6,061,316	3,950,538	65.2%
3	23	Mar. 2020	6,118,607	4,048,714	66.2%
4	24	Mar. 2021	6,232,307	3,781,640	60.7%
5	25	Nov. 2022	6,426,211	4,084,119	63.6%

4.2 Geographic Data

Municipal boundary polygons were obtained from the Israel CBS geographic databases [Israel Central Bureau of Statistics, 2023b] in Shapefile format. Municipalities were dissolved from locality-level polygons to municipality-level using an official locality-to-municipality mapping. The resulting GeoJSON file contains 234 polygon features, of which 229 are consistently matchable across all five elections.

4.3 Party-to-Bloc Mapping

Israeli political parties were classified into five political blocs, as shown in Table 2.

Table 2: Party-to-bloc classification.

Bloc	Description	Example Parties
Right	Nationalist-secular right	Likud, Yisrael Beiteinu, Religious Zionism
Haredi	Ultra-Orthodox religious	Shas, United Torah Judaism
Center	Centrist parties	Yesh Atid, Blue and White
Left	Labor-left	Labor, Meretz
Arab	Arab-majority parties	Joint List, Ra'am, Balad

4.4 Data Processing Pipeline

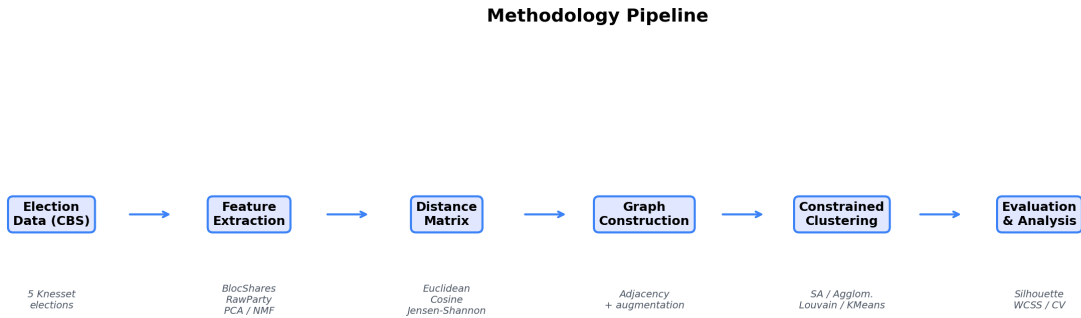


Figure 1: End-to-end methodology pipeline from raw election data to evaluated canton partitions.

The data processing pipeline (Figure 1) handles: (1) loading raw election files and geographic shapefiles; (2) name normalization for cross-dataset matching; (3) municipality dissolution from locality-level to municipality-level polygons; and (4) feature computation from raw vote counts to vote share vectors.

5 Methodology

5.1 Feature Representations

We evaluate four feature representations for municipality political profiles:

BlocShares (11 features): For each municipality, compute the mean and standard deviation of each bloc’s vote share across all five elections, plus the average voter count. This produces an 11-dimensional vector capturing both the political profile and its temporal stability.

RawParty (high-dimensional): The full vector of party-level vote shares, averaged across elections. This preserves fine-grained political distinctions but is high-dimensional and noisy.

PCA_5 (5 features): Five principal components extracted from the RawParty representation via PCA [Jolliffe, 2002], capturing the dominant axes of political variation.

NMF_5 (5 features): Five components from Non-negative Matrix Factorization [Lee and Seung, 1999] of the RawParty representation, producing additive, non-negative components interpretable as political archetypes.

5.2 Distance Metrics

Three distance metrics measure political dissimilarity between municipalities:

Euclidean Distance: The standard L_2 norm between feature vectors. Sensitive to magnitude differences.

Cosine Distance: Measures angular distance between feature vectors ($1 - \cos \theta$). Invariant to vector magnitude, focusing on relative proportions rather than scale.

Jensen-Shannon Distance: The square root of the Jensen-Shannon divergence [Lin, 1991], a symmetric, bounded measure for probability distributions:

$$\text{JSD}(P\|Q) = \frac{1}{2}D_{KL}(P\|M) + \frac{1}{2}D_{KL}(Q\|M), \quad M = \frac{1}{2}(P + Q) \quad (2)$$

Our implementation uses $d(P, Q) = \sqrt{\text{JSD}(P\|Q)}$ (Eq. 2), which is a proper metric [Endres and Schindelin, 2003].

5.3 Graph Construction and Preprocessing

We construct a contiguity graph $G = (V, E)$ where municipalities are nodes and edges connect municipalities sharing a geographic boundary. The raw graph has 234 nodes and 516 edges but is *disconnected*. To ensure a connected graph, we apply three preprocessing steps:

1. **Virtual edges for isolates:** For each isolated node, connect it to its $k = 3$ nearest neighbors in feature space.
2. **Enclave edges:** For municipalities where a single bloc exceeds 70% of votes, add edges connecting all enclaves of the same bloc type.
3. **Bridge edges:** For remaining disconnected components, connect each to the largest component via the most politically similar pair.

After subsetting to the 229 analysis municipalities (488 edges), augmentation produces a fully connected graph with 229 nodes and 2,178 edges.

5.4 Clustering Algorithms

Simulated Annealing (SA): SA optimizes the multi-objective cost function (Eq. 1) over the partition space. Starting from a seed-based initialization (each canton is seeded with the municipality having the highest vote share for the corresponding political bloc), the algorithm proposes moves by reassigning a border municipality to an adjacent canton. Moves that improve the cost are always accepted; moves that increase cost by Δ are accepted with probability $\exp(-\Delta/T)$ (Metropolis criterion [Kirkpatrick et al., 1983]), where T is the current temperature. Moves that would break contiguity are rejected. Parameters: initial temperature $T_0 = 1.0$, cooling rate 0.9995, 5,000 iterations per configuration (a grid-search budget constraint; see Section 9 for a 50,000-iteration sensitivity analysis).

Agglomerative Clustering: Average-linkage with contiguity constraints [Murtagh and Legendre, 2014]—starting from 229 singleton clusters, iteratively merge the two adjacent clusters with the smallest average pairwise distance. Deterministic and contiguity-preserving by construction.

Louvain Community Detection: Maximizes modularity [Newman and Girvan, 2004, Blondel et al., 2008] on the adjacency graph with edge weights derived from political similarity: $w(u, v) = 1 - d(u, v)/d_{\max}$, where d is the chosen distance metric. Louvain does not directly accept a target K ; our implementation performs a binary search over the resolution parameter $r \in [0.01, 10.0]$ (up to 30 iterations, tolerance 10^{-6}) to find the resolution that produces the number of communities closest to the desired K .

K-Means Baseline: Standard K-Means [Hastie et al., 2009] in feature space without geographic constraints. Cantons may be geographically disconnected.

5.5 Evaluation Metrics

Silhouette Score [Rousseeuw, 1987]: Measures how well each municipality fits in its assigned canton versus the nearest alternative. Ranges from -1 to $+1$.

Within-Canton Sum of Squares (WCSS): Total political variance within cantons, $\text{WCSS} = \sum_k \sum_{i \in C_k} \|\mathbf{f}_i - \boldsymbol{\mu}_k\|^2$. WCSS trends closely follow silhouette scores; we report silhouette as the primary quality metric for conciseness.

Population Balance (CV): Coefficient of variation of canton voter populations.

Contiguity: Number of cantons that are disconnected in the adjacency graph. All graph-based algorithms (SA, Agglomerative, Louvain) enforce contiguity by construction. K-Means, operating without geographic constraints, produces disconnected cantons in the majority of configurations.

All algorithms were implemented in Python using scikit-learn [Pedregosa et al., 2011], NetworkX [Hagberg et al., 2008], and SciPy [Virtanen et al., 2020].

6 Experimental Results

6.1 Experimental Setup

We conducted a systematic grid search over 264 configurations (Table 3):

Table 3: Experimental grid dimensions.

Dimension	Values	Count
Representation	BlocShares, RawParty, PCA_5, NMF_5	4
Distance Metric	Euclidean, Cosine, Jensen-Shannon	3
Algorithm	SA, Agglomerative, Louvain, K-Means	4
K (cantons)	3, 5, 7, 10, 15, 20	6
Total	$4 \times 3 \times 4 \times 6 = 288$ minus 24 excluded*	264

*Jensen-Shannon divergence requires non-negative inputs and is incompatible with PCA_5 (which produces negative values); all 24 PCA_5/JSD combinations are excluded.

All 264 configurations executed successfully with 0 failures.

6.2 Key Findings

Representation Comparison: BlocShares achieves the highest silhouette scores for unconstrained algorithms (Figure 3), thanks to its domain-informed aggregation. However, with contiguity-constrained SA, BlocShares produces severely imbalanced partitions. Higher-dimensional representations (NMF_5, RawParty) capture finer-grained political distinctions [Lee and Seung, 1999] and produce better-balanced partitions. RawParty, despite containing the most information, suffers from the curse of dimensionality [Bellman, 1961].

Distance Metric Comparison: Euclidean distance produces the highest silhouette overall (0.905 with BlocShares/Agglomerative at $K = 3$). K-Means baseline achieves 0.858 at $K = 3$ identically across all three metrics, indicating BlocShares features are robust to metric choice for unconstrained clustering.

Algorithm Comparison:

- **Agglomerative** achieves the highest silhouette scores (up to 0.905) but can produce severe population imbalance.
- **SA** produces the most balanced cantons due to its explicit population balance objective, at the cost of lower silhouette scores.
- **Louvain** finds its own natural community count; perfectly stable across elections.
- **K-Means** achieves competitive silhouette scores but produces geographically disconnected cantons.

Effect of K : For unconstrained and agglomerative algorithms, silhouette scores [Rousseeuw, 1987] peak at low K values ($K = 3$ or $K = 5$), as shown in Figure 2, suggesting that Israel’s political geography is naturally structured into a small number of macro-regions. SA and Louvain produce lower silhouette scores across all K , reflecting the cost of enforcing contiguity and population balance constraints.

6.3 Best Configurations

Table 4 presents the best result per algorithm family.

6.4 Primary Result: $K = 5$ Louvain Partition

We select $K = 5$ with NMF_5/Cosine/Louvain as the primary result for interpretive analysis based on four criteria (Table 5):

$K = 5$ Louvain wins on 3 of 4 criteria. The silhouette gap between $K = 3$ Agglomerative (0.905) and $K = 5$ Louvain (0.121) is substantial: the $K = 3$ partition achieves high silhouette by collapsing Israel into just three macro-regions (broadly: Jewish-left/center, Jewish-right, Arab), which is well-separated but too coarse to capture the politically meaningful distinction between center-metropolitan and right-periphery Jewish communities. The positive silhouette of $K = 5$ (0.121) indicates weak but above-chance cluster structure, while providing the granularity needed

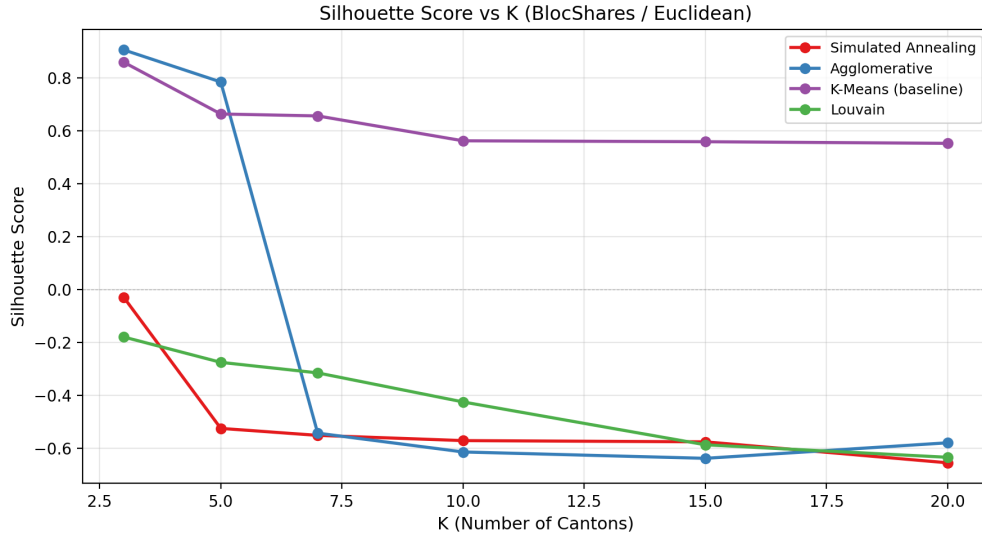


Figure 2: Silhouette score vs K for BlocShares/Euclidean across all four algorithms.

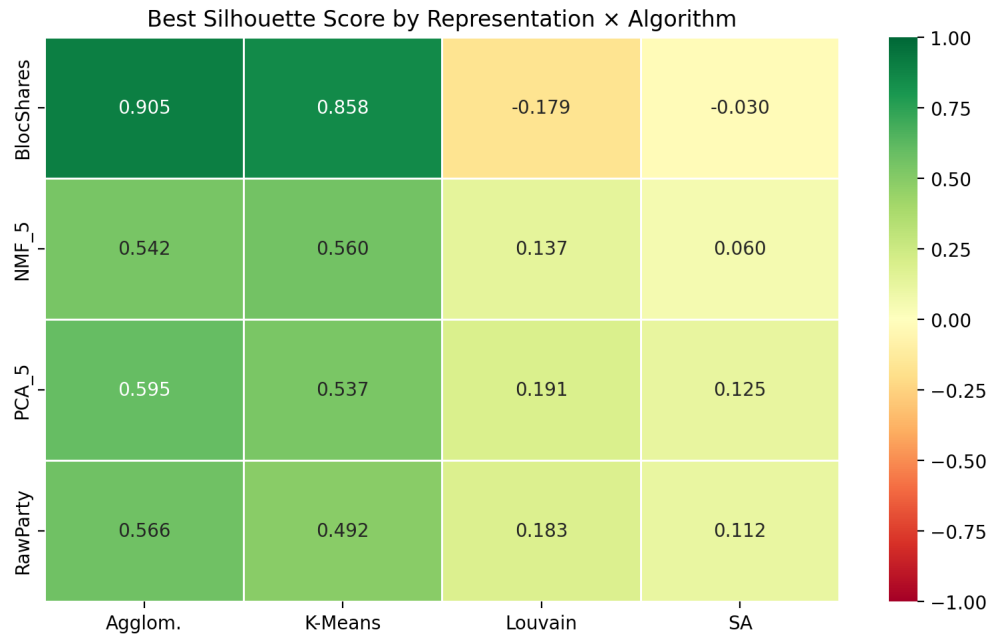


Figure 3: Best silhouette score achieved by each representation \times algorithm combination.

Table 4: Selected configurations: best result per algorithm family.

Rank	Repr	Metric	Algorithm	K	Silhouette	Pop CV
1	BlocShares	Euclidean	Agglomerative	3	0.905	1.13
2	BlocShares	Euclidean	K-Means	3	0.858	0.48
3	NMF_5	Euclidean	Agglomerative	3	0.542	1.14
4	NMF_5	Cosine	Louvain	5	0.121	0.69
5	NMF_5	Cosine	SA	5	-0.042*	0.33*

*SA values are 30-seed means (single run: Sil=-0.015, CV=0.54); see Section 9 for seed sensitivity analysis.

Table 5: Selection criteria for primary result.

Criterion	$K = 3$ Agglom	$K = 5$ Louvain	Winner
Silhouette (higher = better)	0.905	0.121	$K = 3$
Population Balance CV (lower = better)	1.13	0.69	$K = 5$
Temporal Stability ARI (higher = better)	0.954 [†]	1.000	$K = 5$
Political Granularity ($5 > 3$ cantons)	3	5	$K = 5$

BlocShares/Cosine/Agglomerative (nearest tested configuration).

to distinguish CENTER, RIGHT (South/North), and ARAB (Galilee/Periphery) political regions—a five-way split that better reflects Israel’s known political geography. Table 6 presents the canton profiles, Figure 4 shows the geographic partition, and Figure 5 displays the political bloc composition of each canton.

 Table 6: $K = 5$ canton profiles (NMF_5 / Cosine / Louvain). Bloc values are mean vote share (%).

Canton	Munis	Right%	Haredi%	Center%	Left%	Arab%
0 – CENTER Metro	34	29.7	14.4	42.0	11.0	1.1
1 – RIGHT South	60	44.9	10.8	30.0	10.3	1.0
2 – RIGHT North	76	38.0	6.9	31.2	10.9	10.4
3 – ARAB Galilee	43	1.9	1.1	2.2	3.8	89.9
4 – ARAB Periphery	16	2.2	1.0	4.3	5.0	86.1

The two Arab cantons are highly cohesive (89.9% and 86.1% Arab vote share). The two Right cantons differ in character: Canton 1 (RIGHT South) is the southern periphery arc from Jerusalem through the Negev (44.9% Right, 10.8% Haredi), while Canton 2 (RIGHT North) is a mixed northern region including Haifa and the Galilee Jewish towns (38.0% Right). Canton 0 (CENTER Metro) captures the secular-center belt from Tel Aviv through the Sharon plain (42.0% Center).

7 Stability Analysis

7.1 Methodology

To assess whether canton boundaries are structurally stable, we perform temporal stability analysis. For a fixed configuration, we run clustering independently on each of the five elections and measure pairwise agreement using the Adjusted Rand Index (ARI) [Hubert and Arabie, 1985] and Normalized Mutual Information (NMI) [Strehl and Ghosh, 2002].

7.2 Results

Table 7: Cross-election stability for six representative configurations.

Repr	Metric	Algorithm	Mean ARI	Std ARI	Mean NMI	Std NMI
BlocShares	Euclidean	Louvain	1.000	0.000	1.000	0.000
BlocShares	Cosine	Agglomerative	0.954	0.059	0.945	0.071
NMF_5	Euclidean	SA	0.616	0.233	0.682	0.155
BlocShares	Euclidean	SA	0.554	0.113	0.602	0.095
RawParty	Cosine	SA	0.451	0.120	0.550	0.099
PCA_5	Euclidean	SA	0.360	0.137	0.466	0.123

7.3 Interpretation

Deterministic algorithms produce highly stable partitions (Table 7). Louvain produces identical partitions across elections (ARI = 1.0) because it optimizes graph modularity on the fixed adjacency structure with edge weights that change only slightly across elections; this perfect stability reflects algorithmic insensitivity to small feature-space

K=5 Canton Partition (NMF_5 / Cosine / Louvain)

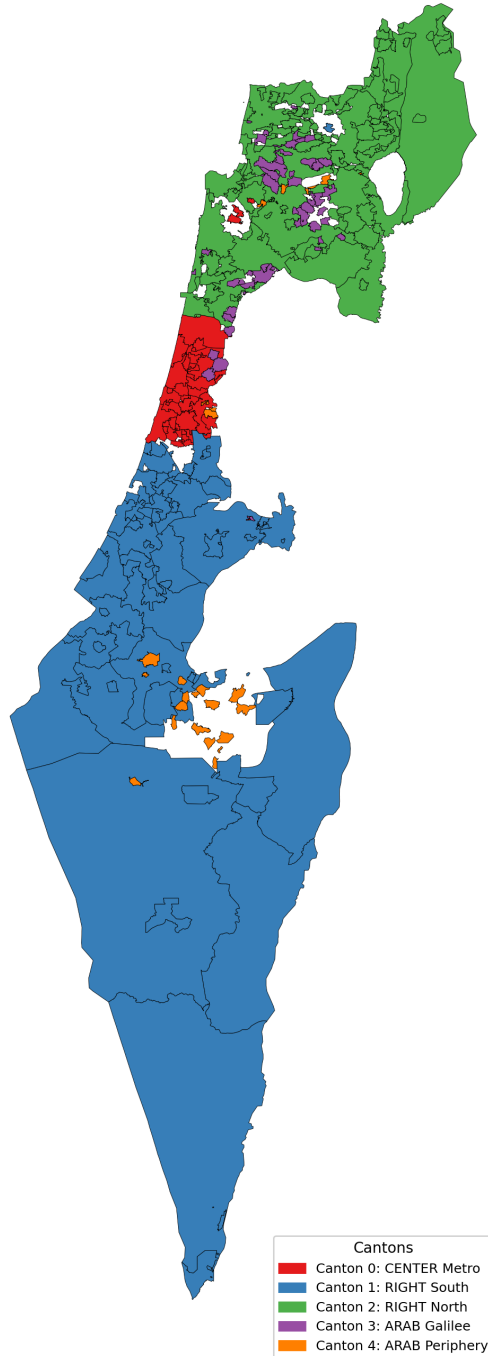


Figure 4: Geographic visualization of the $K = 5$ Louvain canton partition (NMF_5 / Cosine).

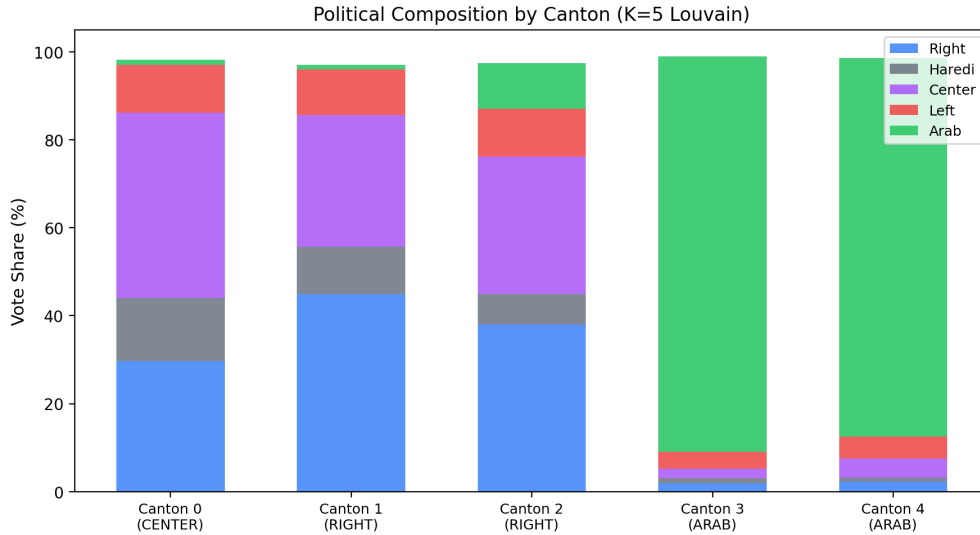


Figure 5: Political bloc composition of each canton in the $K = 5$ Louvain partition.

variations rather than an independent confirmation of geographic structure. Agglomerative clustering produces near-perfect stability ($ARI = 0.954$), which is the stronger evidence for structural persistence since it operates directly on feature-space distances that vary across elections.

SA stability varies by representation. NMF produces the most stable SA partitions ($ARI = 0.616$), followed by BlocShares (0.554). PCA produces the least stable partitions (0.360), likely because principal components rotate across elections as party compositions change.

Overall finding: Over the 2019–2022 period, Israel’s political geography remained structurally consistent across elections (Figure 6). The five elections, despite producing different coalition outcomes, exhibit remarkably similar spatial patterns at the municipality level—consistent with the observation that political preferences are strongly spatially autocorrelated [Anselin, 1995].

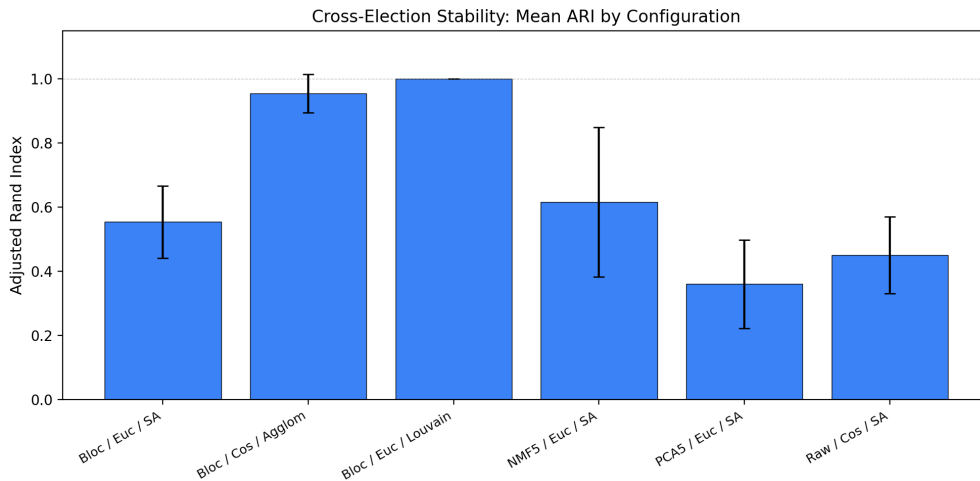


Figure 6: Mean ARI across election pairs for each configuration, with error bars showing standard deviation.

8 Case Studies

We examine five case study areas to assess whether the algorithmic cantons align with known political geography.

8.1 Greater Tel Aviv (Gush Dan)

The secular center-leaning core—Tel Aviv, Ramat Gan, Givatayim, Herzliya, Ra’anana, Kfar Saba, Netanya—is placed in Canton 0 (CENTER Metro, 42.0% Center). Holon, Bat Yam, and Rishon LeZion fall into Canton 1 (RIGHT South), reflecting their right-leaning voting profiles. This split separates the secular-center belt from the right-leaning southern suburbs.

8.2 Jerusalem Region

Jerusalem is placed in Canton 1 (RIGHT South), grouped with Beit Shemesh (both Haredi-dominant), the southern periphery towns, and major southern cities. This canton captures Israel’s right-wing and Haredi heartland (44.9% Right, 10.8% Haredi).

8.3 Arab Towns

The partition produces two distinct Arab cantons: Canton 3 (ARAB Galilee, 89.9% Arab) captures the Galilee and Triangle Arab municipalities, while Canton 4 (ARAB Periphery, 86.1% Arab) captures the Bedouin towns in the Negev and scattered Arab municipalities. This geographic split is politically meaningful: northern Arab municipalities tend to vote for the Joint List, while Bedouin towns have distinct patterns with stronger support for Ra’am [Shamir and Arian, 1999].

8.4 Haifa and the Krayot

Haifa and all the Krayot are assigned to Canton 2 (RIGHT North, 38.0% Right), a large northern canton encompassing the Jewish towns of the Galilee and upper Galilee alongside the Haifa metropolitan area.

8.5 Southern Periphery

All southern periphery towns—Beer Sheva, Dimona, Netivot, Ofakim, Arad, Eilat—are grouped in Canton 1 (RIGHT South, 44.9% Right), forming a contiguous arc from Jerusalem through the Negev to Eilat. This aligns with the well-documented “periphery vote” phenomenon [Arian and Shamir, 2008, Shamir and Arian, 1999].

8.6 Comparison to Administrative Districts

The ARI [Hubert and Arabie, 1985] between our $K = 5$ political cantons and Israel’s official administrative districts is 0.435, confirming that political cantons follow ideological lines rather than administrative boundaries.

9 Limitations and Future Work

9.1 Limitations

Population Imbalance: The $K = 5$ partition has a municipality count range of 16–76 (Pop CV = 0.69). Louvain optimizes modularity rather than balance.

SA Stochasticity: SA results in the grid search use 5,000 iterations per configuration with deterministic seed-based initialization. A 30-seed sensitivity analysis of the primary SA configuration (NMF_5/Cosine/ $K = 5$) using 50,000 iterations showed silhouette scores ranging from -0.141 to 0.035 (mean: -0.042 , std: 0.040) and Pop CV from 0.18 to 0.54 (mean: 0.33 , std: 0.12). This variance is smaller than the gap between SA and Louvain, confirming that algorithmic choice dominates over seed variance.

Ecological Fallacy: Our analysis operates at the municipality level, aggregating individual votes [Robinson, 1950]. Within-municipality variation is not captured.

Static Analysis: We analyze election results as fixed snapshots without modeling demographic shifts or political realignment over time.

Data Coverage: Only 229 of Israel’s 250+ municipalities are included; small localities within regional councils are aggregated at the council level.

Selection Bias: With 264 configurations evaluated, reported “best” silhouette scores may be inflated by selection effects. Relative rankings and qualitative patterns are more robust than absolute performance differences.

9.2 Future Work

- **Finer geographic resolution:** Extend analysis to statistical area or neighborhood level within large cities.
- **Coalition simulation:** Use canton-level profiles to simulate coalition formation under hypothetical regional representation.
- **Cross-country comparison:** Apply the methodology to other countries with spatial political polarization (e.g., United States, Belgium).
- **Temporal dynamics:** Model how canton boundaries shift over time as demographics change.
- **Parameter sensitivity:** Systematic sensitivity analysis of SA cost function weights and graph preprocessing thresholds.

10 Ethical Considerations

This work is purely descriptive and exploratory. The “canton” partitions produced by our algorithms are analytical constructs designed to reveal spatial patterns in voting data; they do not constitute a political proposal or recommendation for territorial division. All data used are publicly available, aggregated at the municipality level, and contain no individual-level information. Readers should be aware of the ecological fallacy [Robinson, 1950]: municipality-level vote shares do not reflect the preferences of any individual voter.

11 Conclusion

This paper demonstrates that constrained spatial clustering can partition Israeli municipalities into politically coherent, geographically contiguous cantons that align with known political-demographic divisions. Our systematic experimental framework—evaluating 264 configurations—provides comprehensive evidence that:

1. **Israel’s political geography is structurally robust.** BlocShares achieves the highest silhouette scores for unconstrained algorithms, while NMF_5 with Louvain produces the most interpretable partition with positive silhouette (0.121) and perfect temporal stability (ARI = 1.0).
2. **The Arab-Jewish divide is the dominant political-geographic cleavage.** In virtually all configurations, Arab-majority municipalities form a distinct, cohesive cluster.
3. **Political cantons differ from administrative districts.** With ARI = 0.435 between our $K = 5$ cantons and administrative districts, political geography follows ideological lines rather than administrative boundaries.
4. **Multi-objective optimization is essential.** Louvain produces the most interpretable partitions with the best balance of silhouette, stability, and political coherence among community detection methods, while SA achieves the best population balance through its explicit multi-objective cost function.
5. **Distance metric choice matters.** Euclidean distance with BlocShares/Agglomerative at $K = 3$ achieves the highest silhouette score (0.905), while the choice of metric interacts with the representation.

This work bridges computer science, geographic information systems, and political analysis, providing both a methodological contribution to constrained spatial clustering and an analytical tool for exploring Israel’s political geography.

Acknowledgments

This work was conducted as part of the first author’s M.Sc. project at the Department of Computer Science, Bar-Ilan University. We thank the Israel Central Bureau of Statistics for making election results and geographic boundary data publicly available.

References

- Nicholas O. Stephanopoulos and Eric M. McGhee. Partisan gerrymandering and the efficiency gap. *University of Chicago Law Review*, 82(2):831–900, 2015.
- Andreas Brieden, Peter Gritzmann, and Fabian Klemm. Constrained clustering via diagrams: A unified theory and its application to electoral district design. arXiv preprint arXiv:1703.02867, 2017.

- Daryl DeFord, Moon Duchin, and Justin Solomon. Recombination: A family of Markov chains for redistricting. *Harvard Data Science Review*, 3(1), 2021.
- Moon Duchin and Bridget Eileen Tenner. Discrete geometry for electoral geography. arXiv preprint arXiv:1808.05860, 2018.
- Trevor Hastie, Robert Tibshirani, and Jerome Friedman. *The Elements of Statistical Learning: Data Mining, Inference, and Prediction*. Springer, 2nd edition, 2009.
- Fionn Murtagh and Pierre Legendre. Ward’s hierarchical agglomerative clustering method: Which algorithms implement Ward’s criterion? *Journal of Classification*, 31(3):274–295, 2014.
- Ulrike von Luxburg. A tutorial on spectral clustering. *Statistics and Computing*, 17(4):395–416, 2007.
- Vincent D. Blondel, Jean-Loup Guillaume, Renaud Lambiotte, and Etienne Lefebvre. Fast unfolding of communities in large networks. *Journal of Statistical Mechanics: Theory and Experiment*, 2008(10):P10008, 2008. doi: 10.1088/1742-5468/2008/10/P10008.
- Mark E. J. Newman and Michelle Girvan. Finding and evaluating community structure in networks. *Physical Review E*, 69(2):026113, 2004. doi: 10.1103/PhysRevE.69.026113.
- Scott Kirkpatrick, C. Daniel Gelatt, and Mario P. Vecchi. Optimization by simulated annealing. *Science*, 220(4598):671–680, 1983. doi: 10.1126/science.220.4598.671.
- Abraham Diskin and Hanna Diskin. The politics of electoral reform in Israel. *International Political Science Review*, 26(1):33–54, 2005.
- Asher Arian and Michal Shamir. A decade later, the world had changed, the cleavage structure remained: Israel 1996–2006. *Party Politics*, 14(6):685–705, 2008.
- Michal Shamir and Asher Arian. Collective identity and electoral competition in Israel. *American Political Science Review*, 93(2):265–277, 1999.
- Luc Anselin. Local indicators of spatial association – LISA. *Geographical Analysis*, 27(2):93–115, 1995.
- Ian T. Jolliffe. *Principal Component Analysis*. Springer, 2nd edition, 2002.
- Daniel D. Lee and H. Sebastian Seung. Learning the parts of objects by non-negative matrix factorization. *Nature*, 401(6755):788–791, 1999. doi: 10.1038/44565.
- Renato M. Assunção, Marcos Corrêa Neves, Gilberto Câmara, and Corina da Costa Freitas. Efficient regionalization techniques for socio-economic geographical units using minimum spanning trees. *International Journal of Geographical Information Science*, 20(7):797–811, 2006.
- Juan C. Duque, Luc Anselin, and Sergio J. Rey. The MAX-P-REGIONS problem. *Journal of Regional Science*, 52(3):397–419, 2012.
- Israel Central Bureau of Statistics. Elections, the Knesset, and government – statistical abstract, 2023a. URL <https://www.cbs.gov.il/en/subjects/Pages/Elections-and-the-Knesset.aspx>. Accessed: 2024.
- Israel Central Bureau of Statistics. Geographic layers – municipal boundaries GIS data, 2023b. URL <https://www.cbs.gov.il/he/Pages/geo-layers.aspx>. Accessed: 2024.
- Jianhua Lin. Divergence measures based on the Shannon entropy. *IEEE Transactions on Information Theory*, 37(1):145–151, 1991.
- Dominik M. Endres and Johannes E. Schindelin. A new metric for probability distributions. *IEEE Transactions on Information Theory*, 49(7):1858–1860, 2003.
- Peter J. Rousseeuw. Silhouettes: A graphical aid to the interpretation and validation of cluster analysis. *Journal of Computational and Applied Mathematics*, 20:53–65, 1987. doi: 10.1016/0377-0427(87)90125-7.
- Fabian Pedregosa, Gaël Varoquaux, Alexandre Gramfort, Vincent Michel, Bertrand Thirion, Olivier Grisel, Mathieu Blondel, Peter Prettenhofer, Ron Weiss, Vincent Dubourg, et al. Scikit-learn: Machine learning in Python. *Journal of Machine Learning Research*, 12:2825–2830, 2011.
- Aric A. Hagberg, Daniel A. Schult, and Pieter J. Swart. Exploring network structure, dynamics, and function using NetworkX. In *Proceedings of the 7th Python in Science Conference (SciPy)*, pages 11–15, 2008.
- Pauli Virtanen, Ralf Gommers, Travis E. Oliphant, Matt Haberland, Tyler Reddy, David Cournapeau, Evgeni Burovski, Pearu Peterson, Warren Weckesser, Jonathan Bright, et al. SciPy 1.0: Fundamental algorithms for scientific computing in Python. *Nature Methods*, 17:261–272, 2020. doi: 10.1038/s41592-019-0686-2.
- Richard E. Bellman. *Adaptive Control Processes: A Guided Tour*. Princeton University Press, 1961.

Lawrence Hubert and Phipps Arabie. Comparing partitions. *Journal of Classification*, 2(1):193–218, 1985.

Alexander Strehl and Joydeep Ghosh. Cluster ensembles – a knowledge reuse framework for combining multiple partitions. *Journal of Machine Learning Research*, 3:583–617, 2002.

William S. Robinson. Ecological correlations and the behavior of individuals. *American Sociological Review*, 15(3): 351–357, 1950.